International Journal of Advanced Manufacturing Technology, Vol. 25, 2005, pp.1089-1097.

The effects of machining process variables and tooling characterisation on the surface generation: modelling, simulation and application promise

Xichun LUO, Kai CHENG* and Robert WARD

School of Engineering, Leeds Metropolitan University

Calverley Street, Leeds LS1 3HE, UK

Abstract

The paper presents a novel approach for modelling and simulation of the surface generation in the machining process. The approach, by integrating dynamic cutting force model, regenerative vibration model, machining system response model and tool profile model, models the complex surface generation process. Matlab Simulink is used to interactively perform the simulation in a user-friendly, effective and efficient manner. The effects of machining variables and tooling characteristics on the surface generation are investigated through simulations. CNC turning trials have been carried out to evaluate and validate the approach and simulations presented. The proposed approach contributes to comprehensive and better understanding of the machining system, and is promising for industrial applications with

*Correspondence to: Professor Kai Cheng, School of Engineering, Leeds Metropolitan University, Calverley Street, Leeds LS1 3HE, UK
TEL: 0113 283 6731 FAX: 0113 283 3110 E-mail: K. Cheng@lmu.ac.uk

particular reference to the optimisation of the machining process based on the product/component surface functionality requirements.

Key Words: Machining processes, surface generation, modelling and simulation

Nomenclature

C_{ta}	damping coefficient of the tooling system
C_{wa}	damping coefficient of the workpiece system
d_c	depth of cut
D	workpiece diameter
f	feed rate
$F_x(t)$	dynamic cutting force in the X direction
$F_y(t)$	dynamic cutting force in the Y direction
$F_z(t)$	dynamic cutting force in the Z direction
G_{tab}	the corresponding response of the tooling structure in the a-th direction due to the force acting in the b-th direction
G_{wab}	the corresponding response of the workpiece in a-th direction due to the force acting in the b-th direction
i, j	sampling points index on the workpiece along the X and Z directions respectively
K_{ab}	structural stiffness
K_{fc}	cutting force constant contributed by shear action in the feed direction
K_{fe}	edge cutting force constant in the feed direction
K_{ff1}, K_{ff2}	flank face cutting force constants in the feed direction
K_{rc}	cutting force constant contributed by shear action in the radial direction

*Correspondence to: Professor Kai Cheng, School of Engineering, Leeds Metropolitan University, Calverley Street, Leeds LS1 3HE, UK
TEL: 0113 283 6731 FAX: 0113 283 3110 E-mail: K. Cheng@lmu.ac.uk

K_{re}	edge cutting force constant in the radial direction
k_{ta}	structural stiffness of the tooling system
K_{tc}	cutting force constant contributed by shear action in the tangential direction
K_{te}	edge cutting force constant in the tangential direction
K_{tf1}, K_{tf2}	flank face cutting force constants in the tangential direction
k_{wa}	structural stiffness of the workpiece system
m_{ta}	mass of the tooling system
m_{wa}	mass of the workpiece system
M, N	number of the sampling points in the X and Z directions respectively
r	tool nose radius
S_{ku}	kurtosis of the surfaces height distribution
S_q	surface root-mean-square deviation
T	one spindle revolution period
β	side clearance angle
μ	friction coefficient
θ_r	intersection angle for two continuous tool path
ω_{mab}	structural natural frequency
ζ_{ab}	structural damping ratio

1 Introduction

Machining process variables and tooling characteristics are important factors affecting the machining quality and efficiency. The primary method used by the industry to select process parameters and tooling geometry often involves costly, time-consuming and trial-and-error process [1]. Because the performance of a product/component depends on its surface quality, a scientific approach is much needed to get better and scientific understanding of the effects of machining process variables and tooling characteristics and their intrinsic relation with the surface generation.

In principle, the surface roughness model can be deduced from the geometry of the tool profile and cutting feed rate and used to predict the ideal surface roughness [2]. The model should ideally provide useful insight into the generation of machined surfaces and the principal controlling factors. Some numerical simulation methods, such as Finite Element Analysis, are used to calculate the thermo-mechanical variables including temperature, pressure, chip speed and to predict the cutting forces [3]. The response surface method [4] and Neural Network method [5] have been utilized to optimise the machining process variables. However, the generation of a machined surface is a dynamic process in which the machining dynamics and structural dynamics should be fully taken into account so as to ensure the modelling and simulation precise and realistic. There are only few researchers studying the effects of machining process variables and tooling characteristic in the dynamic environment [6] [7].

In this paper, an integrated model is proposed to model the generation of machined surfaces in relation with process variables and tooling characteristics. The modelling is further investigated by simulation and machining trials on a CNC turning machine tool. The paper concludes with a discussion on the potential and applications of this method for the control and optimization of the machining process in particular.

2 Integrated modelling approach

Fig. 1 illustrates the integrated modelling approach which includes dynamic cutting force modelling, regenerative vibration modelling, machining system response modelling and surface topography modelling. The machining variables and tooling characteristics, such as tool rake angle and clearance angle, are inputs to the dynamic cutting force model. The three dimensional cutting forces are generated in the light of the interactions between the cutting tool and workpiece in the cutting zone, which will act on the machine tool and tool structure and make the real tool path away from the ideal tool path. The real tool path can be calculated by the machine tool response model and tooling structural response model. Based on the real tool path, the machined surface can be generated by calculating the intersection points of the tool path sequence. The effects of machining variables and tooling characteristics can therefore be analytically studied on the surface generation to the extent of surface texture, topography and roughness.

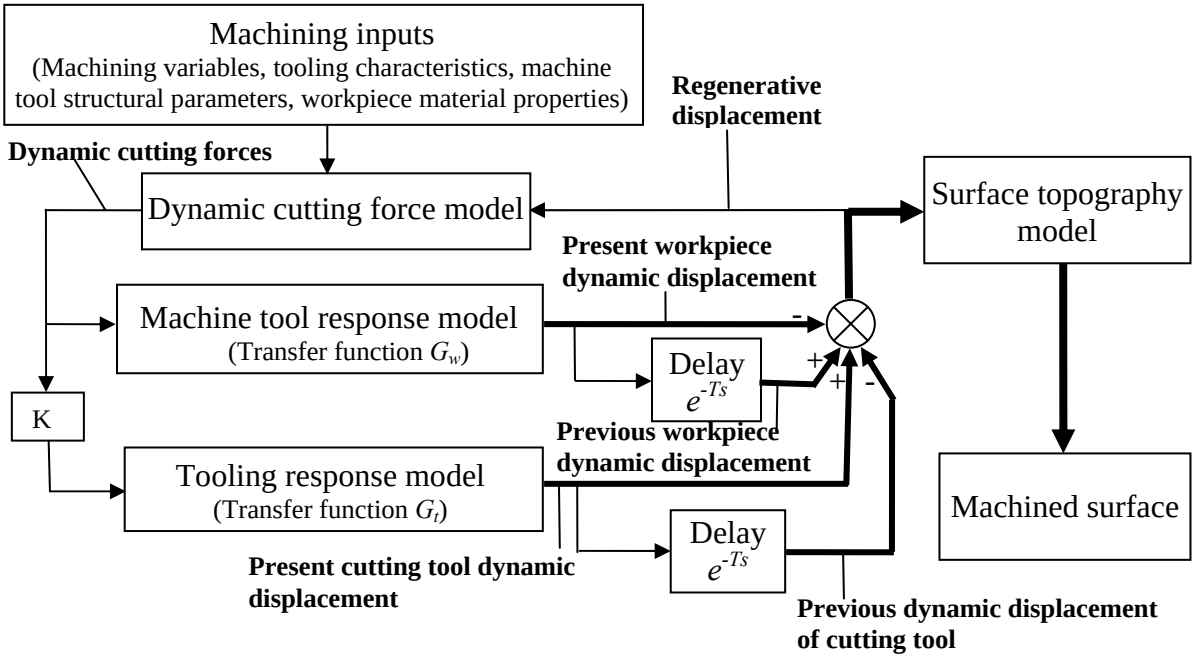

Fig.1 Integrated modelling approach for modelling the surface generation.

Fig. 2 shows the machining dynamics model. The workpiece and cutting tool are simplified as a second-order spring-damper vibratory system in the X, Y and Z directions. The

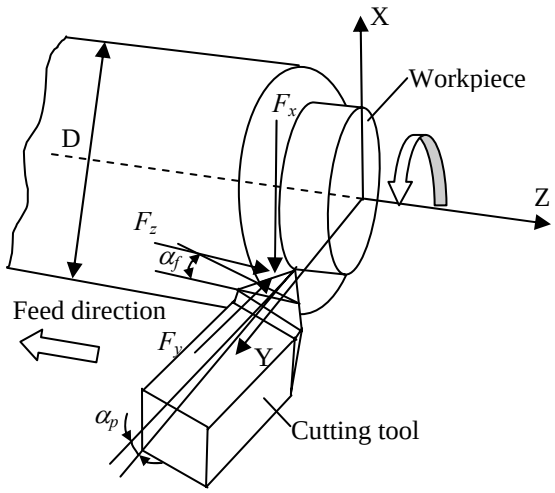

Fig. 2 Machining system diagram.

cutting forces excite the dynamic displacements of the cutting tool and the workpiece in the X, Y and Z directions respectively. The whole cutting system can be described as:

$$\begin{cases} m_{xt}\ddot{xt}(t) + c_{xt}\dot{xt}(t) + k_{xt}xt(t) = F_x(t) \\ m_{yt}\ddot{yt}(t) + c_{yt}\dot{yt}(t) + k_{yt}yt(t) = F_y(t) \\ m_{zt}\ddot{zt}(t) + c_{zt}\dot{zt}(t) + k_{zt}zt(t) = F_z(t) \\ m_{xw}\ddot{xw}(t) + c_{xw}\dot{xw}(t) + k_{xw}xw(t) = -F_x(t) \\ m_{yw}\ddot{yw}(t) + c_{yw}\dot{yw}(t) + k_{yw}yw(t) = -F_y(t) \\ m_{zw}\ddot{zw}(t) + c_{zw}\dot{zw}(t) + k_{zw}zw(t) = -F_z(t) \end{cases} \quad (1)$$

where m_{at}, c_{at}, k_{at}, m_{aw}, c_{aw}, k_{aw} ($a = x, y, z$) are the mass, damping and stiffness of the tooling system and workpiece system in the X, Y and Z directions. It is assumed that m_{xt}, m_{yt}, m_{zt}, m_{xw}, m_{yw} and m_{zw} equal to the mass of the tooling system and workpiece system. F_x(t), F_y(t), F_z(t) are the dynamic cutting forces in the X, Y and Z directions. In the cutting zone, the cutting forces will act on the tool rake face, cutting edge and flank face. Fig. 3 shows the side view and top view of the

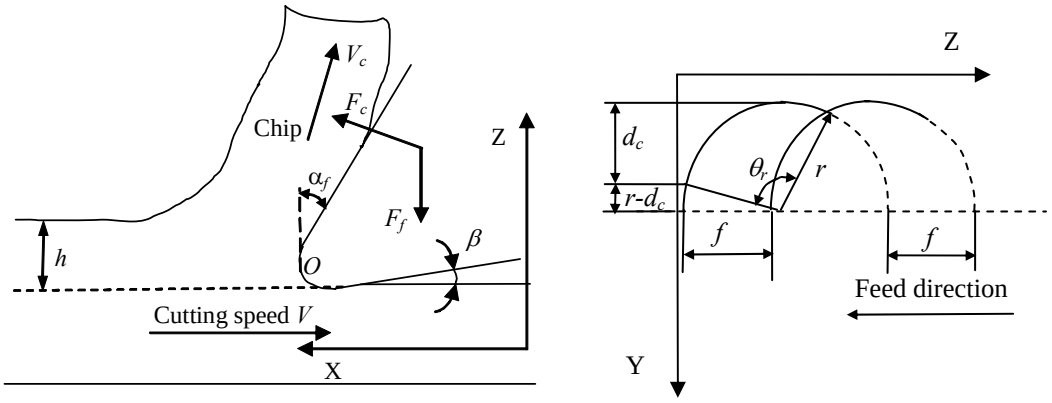

(a) Side view (b) Top view

Fig.3 Tool/workpiece contact area.

tool/workpiece contact area. The forces acted on the rake face can be acquired by the coordinate transformation of the shear plane force based on the shear plane cutting model [6]. The forces acted on cutting edge can be deducted based on the empirical formula of the initial stress and elastic recovery [8]. Accumulating the forces acted on the three zones, there will be the dynamic cutting forces in the three directions expressed as:

$$\begin{cases} F_x(t) = K_{tc}[d_c + y(t+T) - y(t)]\{[h + z(t+T) - z(t)] + \sqrt{r^2 - [r - d_c - y(t+T) + y(t)]^2}\} + K_{te} r\theta_r \\ \qquad + K_{tf1}[\sin(\frac{\beta}{2}) - \mu\cos(\frac{\beta}{2})] + K_{tf2}(\sin\beta - \mu\cos\beta) \\ F_y(t) = (K_{fc} - K_{rc})\sin\theta_r[d_c + y(t+T) - y(t)]\{[h + z(t+T) - z(t)] + \sqrt{r^2 - [r - d_c - y(t+T) + y(t)]^2}\} \\ \qquad + K_{re} r\theta_r \sin\theta_r \\ F_z(\mathrm{t}) = (K_{fc}\sin\theta_r + 1 - \cos\theta_r)[d_c + y(t+T) - y(t)]\{[h + z(t+T) - z(t)] + \sqrt{r^2 - [r - d_c - y(t+T) + y(t)]^2}\} \\ \qquad + (K_{fe}\sin\theta_r + 1 - \cos\theta_r) r\theta_r + K_{ff1}[\cos(\frac{\beta}{2}) + \mu\sin(\frac{\beta}{2})] + K_{ff2}(\cos\beta + \mu\sin\beta) \end{cases} \quad (2)$$

where h is the undeformed chip thickness, which is equal to the feed rate of the cutting tool. f is the feed rate, μ is the friction coefficient, r is the tool nose radius and d_c is the depth of cut. β is the side clearance angle. θ_r is the intersection angle for two continuous tool paths. T is one spindle revolution period. It is worth mentioning that the regenerative vibration will take place in the machining process. It is excited by the cutting forces, as a wavy surface finish left at the previous revolution is removed during the successive revolution, which also leaves a wavy surface owing to the machine structural vibration. It will result in the variation of the chip

thickness and width and excite the variations of the cutting forces vice versa. Hence, the resulting dynamic chip thickness and depth of cut is no longer constants but vary as a function of vibration frequency and the rotational speed of the workpiece. K_{tc}, K_{rc}, $K_{fc,}$ K_{te}, K_{re}, K_{fe}, K_{tf1}, K_{tf2}, K_{ff1} and K_{ff2} are the cutting constants at rake face, cutting edge and flank face in the X and Y and Z directions. They can be acquired by the transformation from the orthogonal cutting experiments and an empirical tool force model [6] [9].

The cutting system model equation (1) can be transformed into frequency domain by Laplace transform, and then further rewritten as:

$$\begin{bmatrix} xt(s) \\ yt(s) \\ zt(s) \\ xw(s) \\ yw(s) \\ zw(s) \end{bmatrix} = (1-e^{-sT}) \begin{bmatrix} G_{xxt} & G_{xyt} & G_{xzt} & 0 & 0 & 0 \\ G_{yxt} & G_{yyt} & G_{yzt} & 0 & 0 & 0 \\ G_{zxt} & G_{zyt} & G_{zzt} & 0 & 0 & 0 \\ 0 & 0 & 0 & G_{xxw} & G_{xyw} & G_{xzw} \\ 0 & 0 & 0 & G_{yxw} & G_{yyw} & G_{yzw} \\ 0 & 0 & 0 & G_{zxw} & G_{zyw} & G_{zzw} \end{bmatrix} \begin{bmatrix} F_x(s) \\ F_y(s) \\ F_z(s) \\ -F_x(s) \\ -F_y(s) \\ -F_z(s) \end{bmatrix} \quad (3)$$

The sub-matrix: $\begin{bmatrix} G_{xxt} & G_{xyt} & G_{xzt} \\ G_{yxt} & G_{yyt} & G_{yzt} \\ G_{zxt} & G_{zyt} & G_{zzt} \end{bmatrix}$ and $\begin{bmatrix} G_{xxw} & G_{xyw} & G_{xzw} \\ G_{yxw} & G_{yyw} & G_{yzw} \\ G_{zxw} & G_{zyw} & G_{zzw} \end{bmatrix}$ are the machine tool response model and the tooling response model for the dynamic cutting force. Where G_{abt} and G_{abw} are the corresponding response of the workpiece/tooling structure in *a*-th direction due to the force acting in the *b*-th direction when the other two force components are zero. *a* and *b* stand for the X/Y/Z direction respectively. Here the assumption of linearity is accepted, i.e. the matrix **G** is symmetric ($G_{ab} = G_{ba}$). The transfer function can be expressed in the form of

$$G_{ab} = \frac{y_{ab}(s)}{F_{ab}(s)} = \frac{\omega_{nab}^2}{K_{ab}(s^2 + 2\zeta_{ab}\omega_{nab}s + \omega_{nab}^2)} \quad (4)$$

where K_{ab} is the structural stiffness, ω_{nab} is the structural natural frequency, ζ_{ab} is the damping ratio of the workpiece and tooling system in *a*-th direction due to a force acting in the *b*-th direction when the other two force components are zero. They can be estimated according to

the tooling/workpiece system structural dimensions and the components specifications provided by the manufacturer.

The relative dynamic displacements between the tool and the workpiece can be determined as:

$$\begin{cases} \Delta x = xt - xw \\ \Delta y = yt - yw \\ \Delta z = zt - zw \end{cases} \tag{5}$$

Superposition of the dynamic displacements with the ideal tool position will be the real tool position onto the workpiece. They can be expressed as:

$$\begin{cases} x_{i,j} = \dfrac{\pi DT}{M}(i-1) + \Delta x_{i.j} \\ y_{i,j} = (D - d_c)\cos(\dfrac{2\pi}{M}i) + \Delta y_{i,j} \quad (i = 1, 2 \ldots M, j = 1, 2, \ldots N) \\ z_{i,j} = -f(j-1) + \dfrac{fT}{M}(i-1) + \Delta z_{i,j} \end{cases} \tag{6}$$

where i and j are the sample points on the workpiece along the X and Z directions. M and N are the number of sample points in the X and Z directions respectively. D is the workpiece diameter.

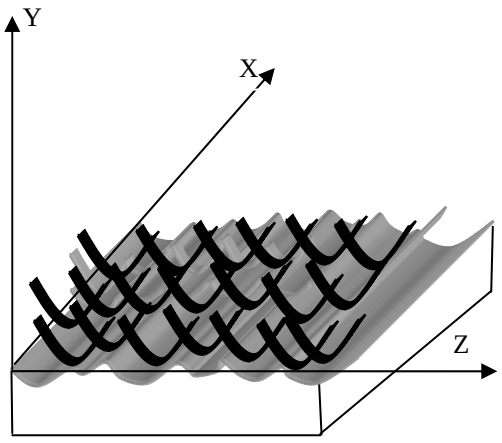

Fig. 4 Surface topography generation model.

The machined surfaces are generated based on the real tool path and tool profile. Fig. 4 illustrates the surface topography model. It is based on the tool profile and the intersection

points of the tool path. The intersection points of the tool path can be calculated by the following equations:

$$\begin{cases} X_{i,j} = \dfrac{x_{i,j} + x_{i+1,j}}{2} \\ Y_{i,j} = y_{i+1,j} + \dfrac{(z_{i,j} - z_{i+1,j})^2}{2r} \\ Z_{i,j} = \dfrac{2r(y_{i,j} - y_{i+1,j}) + x_{i,j}^2 - x_{i+1,j}^2}{2(z_i - z_{i+1})} \end{cases} \quad (i = 1, 2, \ldots, M; j = 1, 2, \ldots, N) \quad (7)$$

Trimming the line above the intersection points, there will be the machined surface.

3 Simulation of the generation of machined surface and experimental validation

The whole machining dynamics model is implemented in a MATLAB simulink environment. It includes the cutting force module and machining system response module. In the simulation, an intervally repeated ramp function is used to emulate the variation of effective rake angle due to the generation of build-up edge and its removal at the tool's rake surface. The frequency of the function is about 5.25 Hz. A delay function is used to represent regenerative vibration effects on the variation of the depth of cut and the feed rate.

Machining trials are carried out on a CNC lathe to validate the model and simulation. The experimental configuration is shown in Fig. 5. The dynamic cutting forces are measured by a Kistler dynamometer, 9257BA, on which the carbide tool insert is mounted. The machined surfaces are measured by the Zygo Newview 5000 optical microscope. The aluminium alloy and steel sample components are machined in the experiments. The machining conditions are listed in Table 1.

Table 1 Machining trial conditions.

Workpiece	Material	Al alloy/Low carbon steel
	Diameter (mm)	ϕ 50
Cutting tool	Material	Carbide insert
	Nose radius (mm)	0.4, 0.6, 0.8, 1.0, 1.2
	Initial side rake angle (°)	0, ± 5
	Side clearance angle (°)	0, 5, 7
	Back rake angle (°)	10
	Back clearance angle (°)	6
Operation conditions	Spindle speed (rpm)	490 ~ 1,400
	Feed rate (mm/rev)	0.0397 ~ 0.3175
	Depth of cut (mm)	0.01, 0.1, 0.5

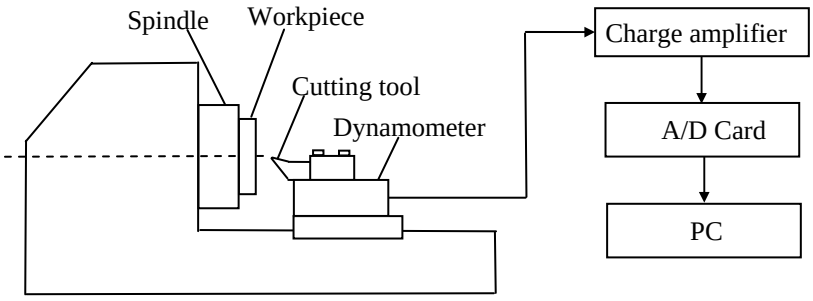

Fig. 5 Experimental configuration of the cutting trials.

Fig.6 shows the simulated and measured cutting forces in the radial direction when the cutting is undertaken at the conditions: spindle speed = 1,400 rpm, feed rate = 0.0397~0.3175 mm/rev and depth of cut = 0.01 mm. It can be seen that the simulated cutting forces are well agreed with the measured results (about 29.8% lower than the measured results). It also shows the tendency that the radial cutting force increases with the increment of the feed rate. When the feed rate 0.0397 mm/rev is applied, the simulated machined surface and the measured surfaces

are shown in Fig 7. The direction of lay is evident in both the simulated

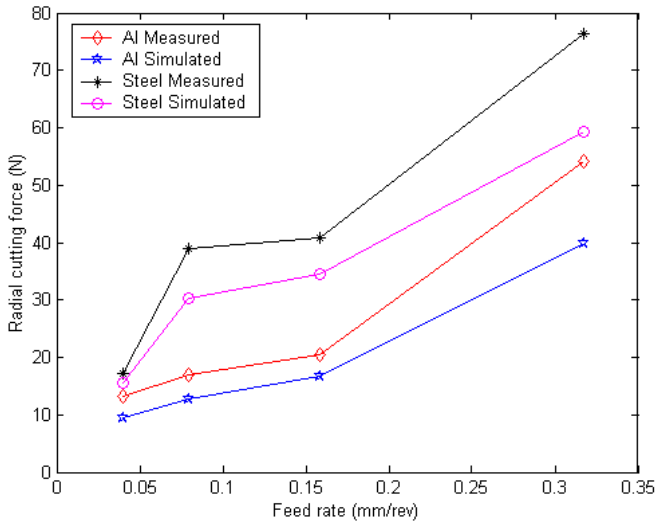

Fig. 6 The variation of the radial cutting forces with different feed rate.

surface and the experimentally generated surface. The root-mean square deviation S_q of the simulated surface is 0.083 μm, which is close to the experimental result 0.14 μm. The difference between the simulation result and experimental result may be caused by the estimated static machining structural parameters. But the simulation results are still in the reasonable deviation scale.

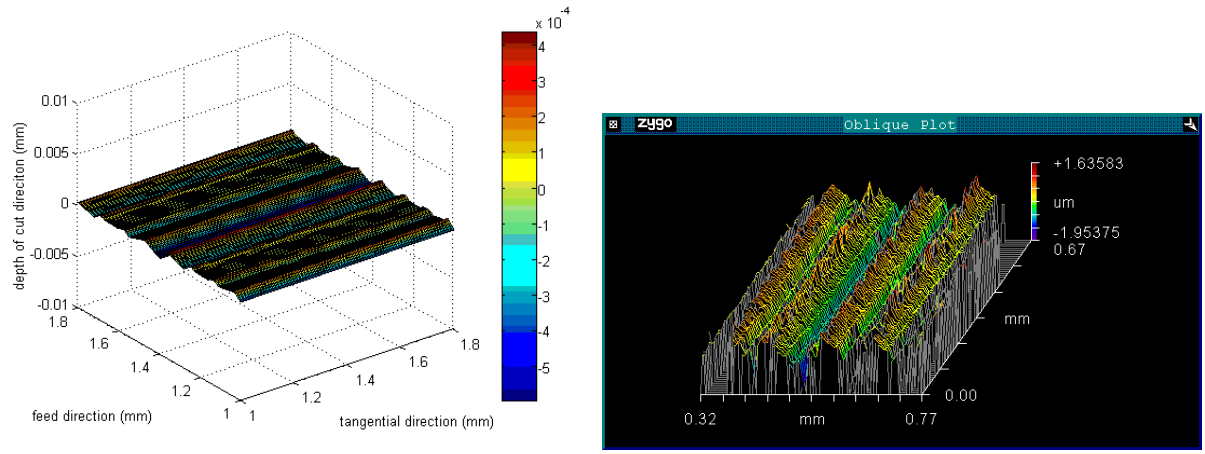

(a) Simulated surface (b) Machined surface

Fig. 7 Comparison between the simulated surface and machined surface.
(f = 0.0397 mm/rev, n = 1,400 rpm, d_c = 0.01 mm, r = 1.2 mm)

4 Discussions

4.1 The effects of the process variables on the machined surfaces

In order to study the effects of the machining conditions on the machined surface, spectral analysis technique is used to characterize the machined surfaces. Fig. 8 shows the area power spectral density of a machined surface. It can be found that the feed rate is the most dominant factor for the machined surfaces. Its frequency is $1/f$= 1/0.1588 = 6.29 cycle/mm. The other significant component is the regenerative vibration, its spatial frequency in the feed rate direction is about 20 cycle/mm. The variation of the rake angle due to the built-up-edge

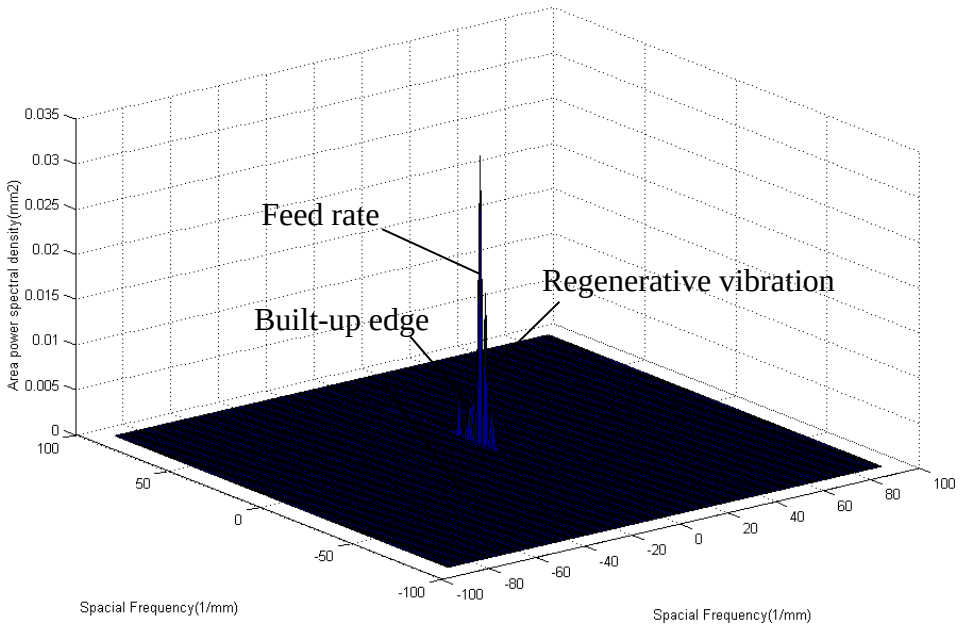

Fig.8 Area power spectral of the machined surfaces.
(f = 0.1588 mm/rev, n = 1,400 rpm, d_c = 0.1 mm, r = 0.4mm)

has lower magnitude of the power spectral density, while it still leaves its mark on the machined surfaces.

The effects of the feed rate and the tool nose radius on the machined surface are studied by simulations and machining trials of cylindrical turning of Al alloy. In the simulations and machining trials, the feed rate varies from 0.0397 mm/rev to 0.3175 mm/rev, the tool nose radius varies from 0.4 mm to 1.2 mm, the depth of cut kept at 1 mm and spindle speed kept at

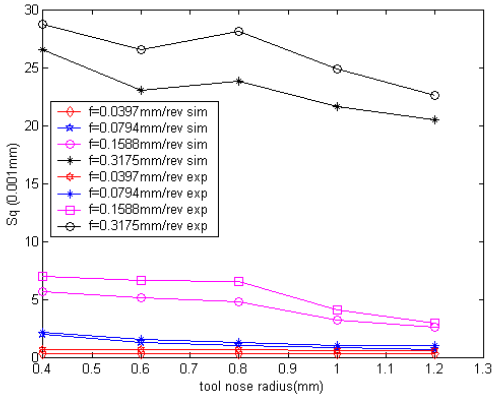

Fig. 9 The effects of feed rate and tool nose radius on the surface roughness.

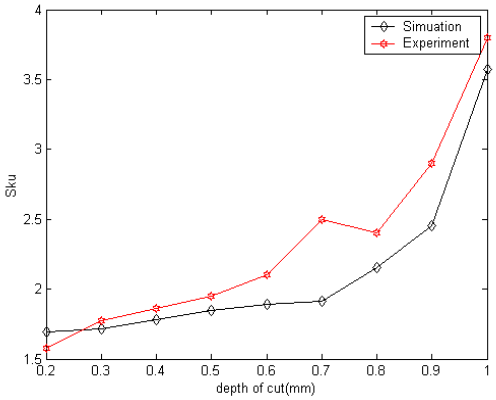

Fig. 10 The effects of depth of cut on the kurtosis of surface height distribution.

1,400 rpm. Fig. 9 illustrates that the feed rate has significant effects on the machined surface roughness. It can be found that the value of surface root-mean-square deviation S_q decreases as decreasing the feed rate. The tendency is consistent with the conventional cutting theory. The decrement of feed rate will decrease the cutting force and then decrease the cutting system vibrations excited by the cutting force, and it can also decrease the distance of the feed mark on the machined surface, so the surface finish is improved when the low feed rate are adopted [10]. The effect of the tool nose radius depends on the feed rate. The surface root-mean-square deviation S_q decreases with the increase of the tool nose radius at low feed rate. The tendency is consistent with the conventional theory [11]. Though at high feed rate S_q decreases with the increase of the tool nose radius in general, there is irregularity at a tool nose radius of 0.8 mm. The S_q value at tool nose radius of 0.8 mm is large and is nearly equal to the S_q value at tool nose radius of 0.4 mm. It can be explained by Shaw's theoretical analysis on surface finish [11]: when the ratio of feed rate (f) to tool nose radius (r) is about between 0.4 and 0.8, the relationship between the ratio of feed rate (f) to tool nose radius (r) and the ratio of average

surface roughness (R_a) to tool nose radius (r) is nearly linear. It is just the case when the tool nose radius of 0.8 mm and 0.4 mm with feed rate 0.3175 mm/rev are used, in which the ratio f/r is 0.39 and 0.794 respectively. Although the ratio R_a/r value of the former is nearly half that of the latter, because its tool nose radius is two times bigger than that of the former, its surface roughness values is nearly equal to that of the latter.

The effects of the depth of cut on the surface height distribution are studied under the same cutting speed, whereas the tool nose radius = 1.2 mm and feed rate = 0.0397 mm/rev respectively. The depth of cut varies from 0.2 to 1.0 mm. Fig. 10 shows the kurtosis of the surface height distribution S_{ku} is very sensitive to the variation of the depth of cut. It can be found that the S_{ku} increases with increasing the depth of cut. It means decreasing the depth of cut will greatly benefit the achievement of the machined surfaces with well spread height distribution.

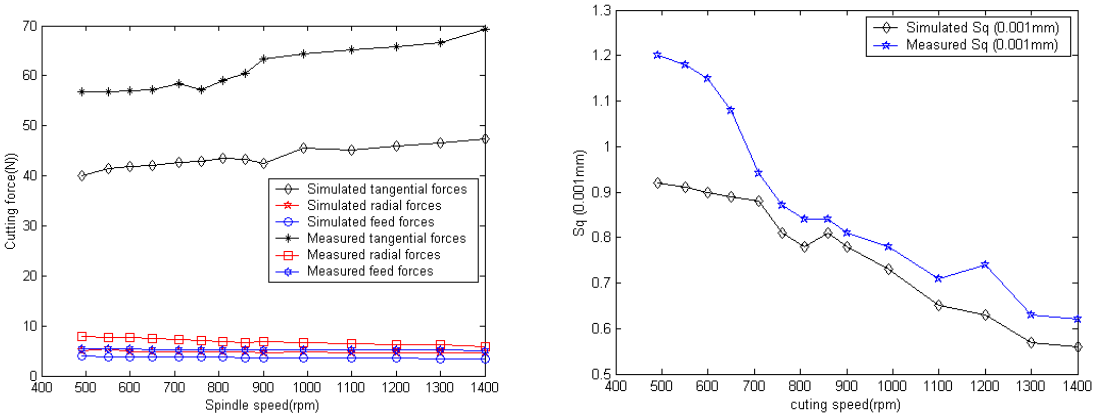

(a) 3D Cutting forces under different spindle speed

(b)The effects of spindle speed on surface roughness

Fig. 11 The effects of the spindle speed on the cutting forces and machined surfaces.

The effects of spindle speed on the cutting forces and the machined surfaces are investigated by the simulation and machining trials of cylindrical turning of Al alloy. The feed rate = 0.0397 mm/rev, depth of cut =0.5 mm, tool nose radius = 1.2 mm. Fig. 11 (a) shows the

tangential cutting force increases with the increase of the spindle speed, whereas the radial and feed cutting forces decrease with the increase of the spindle speed. Fig. 11 (b) shows the surface roughness decreases with the increase of the spindle speed. The trends are consistent with the conventional theory [11]. The radial force is the most dominant force component contributing to the generation of machined surfaces. Therefore, the surface roughness decreases with the increases of the spindle speed.

4.2 The effects of the tooling characteristics

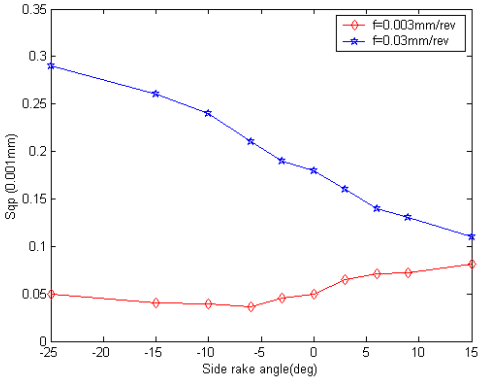

Fig. 12 The effects of side rake angle on the surface roughness.

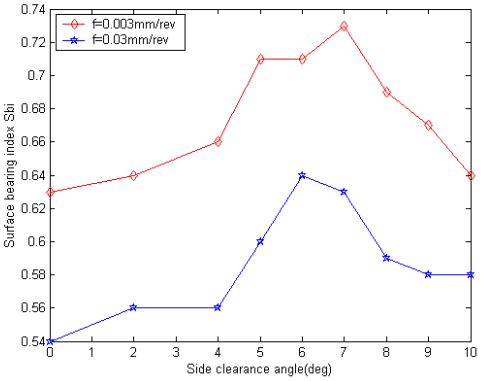

Fig. 13 The effects of side clearance angle on the surface bearing ability.

The relationship between the side rake angle and the surface roughness is studied by simulating the cylindrical turning of Al alloy. In the simulations, spindle speed is set as 1,400 rpm, tool nose radius = 1.2mm, side clearance angle = 5°. The feed rate and depth of cut are 0.003 mm/rev × 0.01 mm and 0.03 mm/rev × 0.1 mm respectively. The former stands for the finish machining, and the latter stands for the rough machining. As shown in Fig. 12, in the finish machining a good surface finish can be achieved with a cutting tool with negative side rake angle (about -5° ~ -15°). It is because in finish machining the proper negative rake angle can provides the necessary hydrostatic pressures to enable plastic deformation of the workpiece material beneath the tool to take place and to sustain plastic flow, and the tensile

stress is smaller than that of using a cutting tool with positive rake angle [12]. In the rough machining, a cutting tool with positive side rake angle will be helpful to decrease the surface roughness. It is because in rough machining positive rake angle makes the cutting force smaller than that of using a cutting tool with negative rake angle, the small cutting force will decrease the cutting system vibrations [11].

The effect of the clearance angle on the surface bearing ability is studied by simulating the cylindrical turning of Al alloy. The similar machining conditions which stand for the finish and rough machining are adopted except the side clearance angle varies from 0° to 10°. Fig. 13 shows when the side clearance angle is about 5° ~ 7° the machined surface with good surface bearing ability can be achieved in both finish and rough machining. Therefore, the 5° ~ 7° side clearance angle enables the elastic recovery and can improve the surface bearing ability of the machined surface.

The effects of the tooling structure on the machined surfaces are studied by two simulations of the face turning of Al alloy. In both simulations, the spindle speed = 1,400 rpm, depth of cut =

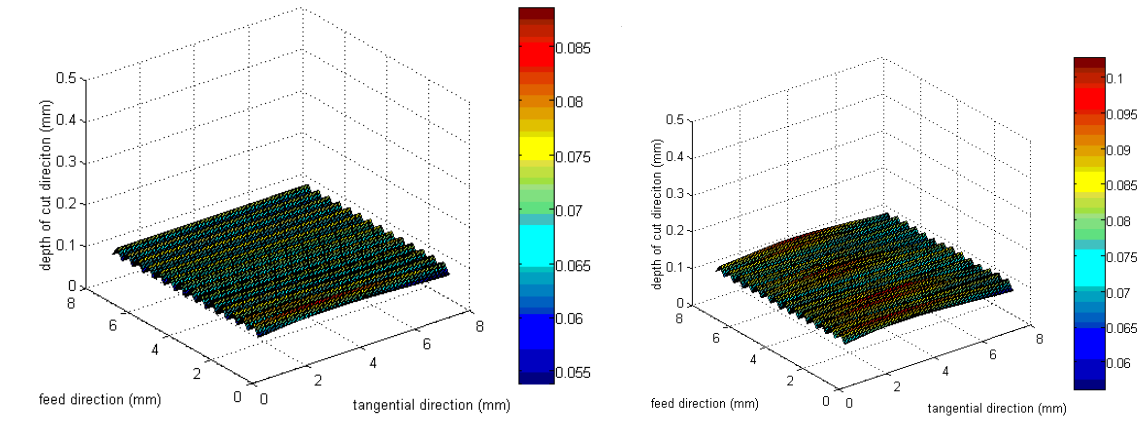

(a) Simulation No.1 (b) Simulation No.2

Fig. 14 The effects of tooling structural characterization on the machined surfaces.

2.0 mm, feed rate = 0.5mm/rev. But in the latter simulation the result of tooling structural stiffness multiplying the damping ratio is one tenth of that of the former. The comparison of the simulated surfaces is shown in Fig. 14. The root-mean square deviations S_q of the machined surfaces are 5.8 μm and 11.6 μm respectively. It can be found that the surface roughness will be degraded because of the bad tooling structural characteristics.

The cylindrical turning trial is carried out with the low preload force on the bolt of the toolholder. The tool insert is observed using the Zygo microscope as shown in Fig. 15, before and after four machining cycles (spindle speed = 1,400 rpm, depth of cut =2 mm, feed rate =0.1588 mm/rev, cutting distance =20mm). Obvious edge chipping can be observed on the tool inserts in Fig. 15 (b), which indicates the bad tooling structural characteristics can result in tool wear.

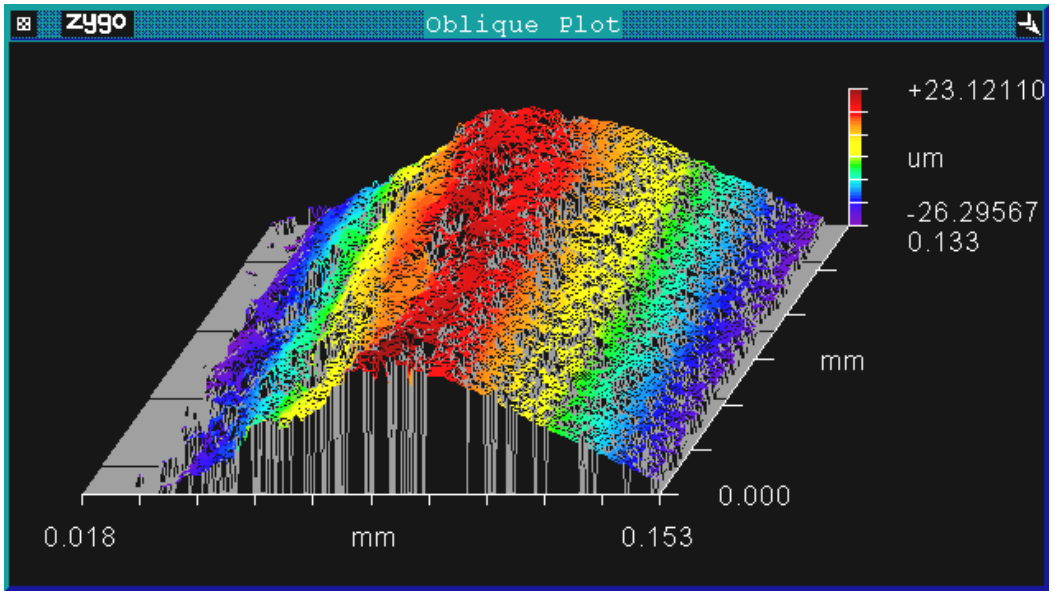

(a) Cutting edge before the cutting trial

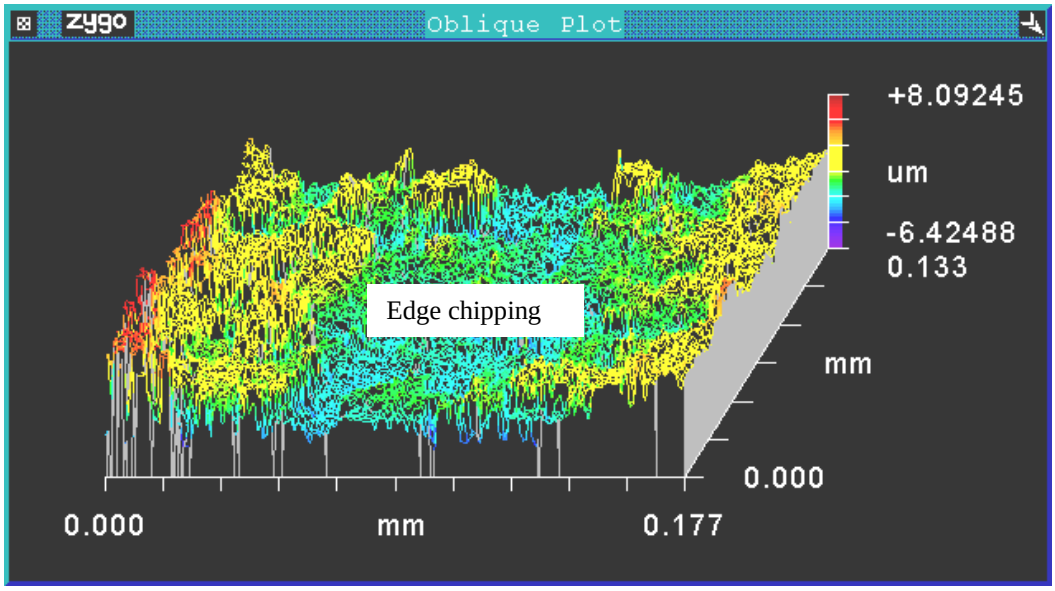

(b) Cutting edge after the cutting trial

Fig. 15 Tool wear due to improper damping.

4.3 Application promise

The experimental trials and simulation results have shown that the modelling and simulation approach enables the in-depth study of the effects of machining variables and tooling characteristics on the machined surfaces generation. It can accurately present the surface dynamic generation process in which the machining dynamics and machining system

structural dynamics are involved. The additional advantage of the technique which distinguishes it from conventional modelling approach is that it is built in an opening interactive programming environment, so some machining factors such as the environmental vibrations and the machine tool errors can be easily added into the model in the form of linear or nonlinear functions with respect to their physical characters. Therefore, the modeling approach and associated simulations developed have the following potentials [13] [14]:

- To be built into the CNC controller as a ‘soft gauge’ to monitor the machining process instability (chatters)
- To optimise the machining process conditions against the component surface functionality as required
- To design the surface (digitally) against its functional performance
- To be used as a generic research tool for the investigation of machining dynamics and machined surfaces generation (turning, milling and grinding processes).

5 Conclusions

An integrated model has been proposed to simulate the surface generation in turning processes. The machined trials show the modelling approach can accurately present the dynamic cutting process and the effects of machining process variables and tooling characteristics. It is found that the feed rate plays the most significant role on the machined surfaces. The decreasing of the depth of cut will greatly benefit the achievement of the machined surfaces with well spread of height distribution. The negative rake angle (about -5°) will be significant for the achievement of good surface finish in finish machining. A proper clearance angle (about 5° ~ 7°) enables the elastic recovery of machined surfaces and can improve the surface bearing ability of the machined surfaces. The tooling structural characteristics are significant for the machined surface accuracy. Bad tooling structure can

result in the tool wear and degrade the machined surface accuracy. The approach and simulations are very promising for industrial applications with particular reference to the optimisation of the machining process based on the product/component surface functionality requirements.

Acknowledgments

The authors would like to thank Kistler (UK) Ltd for their support and assistance of this research.

References:

[1] K. Taraman and B. Lambert, “A surface roughness model for a turning operation”, International Journal of Production Research, 12(6), pp. 691-703, 1974.

[2] D. J. Whitehouse, Handbook of Surface Metrology, Institute of Physics Publishing, Bristol, 1994.

[3] T. Moriwaki, N. Sugimura and S. Luan, “Combined stress, material flow and analysis of orthogonal micromachining of Copper”, Annals of the CIRP, 42(1), pp. 75-78, 1993.

[4] J. S. Baras and N. S. Patel, “Designing response surface model-based run-by-run controllers: a worst case approach”, IEEE Transactions on Components, Packaging & Manufacturing Technology, Part C Manufacturing, 19(2), pp. 98-104, 1996.

[5] R. K. Iain and V. K. Jain, “Optimum selection of machining conditions in abrasive flow machining using neural network”, Journal of Materials Processing Technology, 108 (1), pp. 62-67, 2000.

[6] Y. Altintas, Manufacturing Automation: Metal Cutting Mechanics, Machine Tool Vibrations, and CNC Design, Cambridge University Press, Cambridge, 2000.

[7] C. F. Cheung and W. B. Lee, “Characterisation of nanosurface generation in single-point diamond turning”, International Journal of Machine Tools & Manufacture, 41, pp. 851-875,

2001.

[8] C. Arcona and T. A. Dow, “An empirical tool force model for precision machining”, Transactions of the ASME: Journal of Manufacturing Science and Engineering, 120, pp. 700-707, 1998.

[9] X. Fan and M. H. Miller, “The application of an empirical tool force model on vibration cutting”, Proceedings, 17th ASPE Annual Meeting, St. Louis, USA, pp. 484-489, 20-25 October, 2002.

[10] E. J. A. Armarego and R. H. Brown, The Machining of Metals, Prentice-Hall, Englewood Cliff, NJ, 1969.

[11] M. C. Shaw, Metal Cutting Principles, Oxford University Press, Oxford, 1984.

[12] R. Komanduri, N. Chandrasekaran and L. M. Raff, “Effect of tool geometry in nanometric cutting: a molecular dynamics simulation approach”, Wear, 219, pp. 84-97, 1998.

[13] X. K. Luo, K. Cheng and X. C. Luo, “A simulated investigation on machining instability and non-linear aspects in CNC tuning processes”, The International Journal for Manufacturing Science & Production, 5(1-2), pp. 45-50, 2003.

[14] K. Cheng, X. C. Luo and X. K. Luo, “A simulated investigation on the surface functionalities in precision machining processes”, Proceedings, 18th International Conference on Computer-Aided Production Engineering (CAPE 2003), Edinburgh, UK, pp. 385-394, 18-19 March, 2003.